Title
Evaluation and improvements of two community models in simulating dry deposition velocities for peroxyacetyl nitrate (PAN) over a coniferous forest

Journal
Journal of Geophysical Research, 117(D4)

ISSN
0148-0227

Authors
Wu, Zhiyong
Wang, Xuemei
Turnipseed, Andrew A
et al.

Publication Date
2012-02-27

DOI
10.1029/2011jd016751

Evaluation and improvements of two community models in simulating dry deposition velocities for peroxyacetyl nitrate (PAN) over a coniferous forest

Zhiyong Wu,[1] Xuemei Wang,[1] Andrew A. Turnipseed,[2] Fei Chen,[2] Leiming Zhang,[3] Alex B. Guenther,[2] Thomas Karl,[2] L. G. Huey,[4] Dev Niyogi,[5] Beicheng Xia,[1] and Kiran Alapaty[6]

Received 19 August 2011; revised 30 November 2011; accepted 30 December 2011; published 29 February 2012.

[1] Dry deposition velocities (V_d) for peroxyacetyl nitrate (PAN) calculated using two community dry deposition models with different treatments of both stomatal and nonstomatal uptakes were evaluated using measurements of PAN eddy covariance fluxes over a Loblolly pine forest in July 2003. The observed daytime maximum of $V_d(PAN)$ was $\sim$1.0 cm s^{-1} on average, while the estimates by the WRF-Chem dry deposition module (WDDM) and the Noah land surface model coupled with a photosynthesis-based Gas Exchange Model (Noah-GEM) were only 0.2 cm s^{-1} and 0.6 cm s^{-1}, respectively. The observations also showed considerable PAN deposition at night with typical V_d values of 0.2–0.6 cm s^{-1}, while the estimated values from both models were less than 0.1 cm s^{-1}. Noah-GEM modeled more realistic stomatal resistance (R_s) than WDDM, as compared with observations of water vapor exchange fluxes. The poor performance of WDDM for stomatal uptake is mainly due to its lack of dependence on leaf area index. Thermal decomposition was found to be relatively unimportant for measured PAN fluxes as shown by the lack of a relationship between measured total surface conductance and temperature. Thus, a large part of the underprediction in V_d from both models should be caused by the underestimation of nonstomatal uptake, in particular, the cuticle uptake. Sensitivity tests on both stomatal and nonstomatal resistances terms were conducted and some recommendations were provided.

Citation: Wu, Z., et al. (2012), Evaluation and improvements of two community models in simulating dry deposition velocities for peroxyacetyl nitrate (PAN) over a coniferous forest, *J. Geophys. Res.*, *117*, D04310, doi:10.1029/2011JD016751.

1. Introduction

[2] Peroxyacetyl nitrate (PAN, $CH_3C(O)OONO_2$) is an abundant secondary pollutant of photochemical oxidation, which is produced in the atmosphere by reactions 1 and 2f:

$$\text{(R1)} \qquad CH_3CHO + OH \xrightarrow{O_2} CH_3C(O)OO + H_2O,$$

$$\text{(R2f, R2r)} \qquad CH_3C(O)OO + NO_2 \rightleftharpoons CH_3C(O)OONO_2.$$

The reverse reaction (R2r) represents the thermal decomposition of PAN, a process highly sensitive to temperature. The reaction of the peroxyacetyl radical (PA, $CH_3C(O)OO$) with NO is the primary removal mechanism of PAN from the atmosphere:

$$\text{(R3)} \qquad CH_3C(O)OO + NO \rightarrow CH_3C(O)O + NO_2.$$

Other chemical decay mechanisms for PAN, including oxidation by hydroxyl radical (OH) and photolysis, are relatively slow and negligible relative to thermal decomposition in the lower troposphere [*Singh*, 1987; *Talukdar et al.*, 1995].

[3] PAN acts as an important reservoir of reactive nitrogen and plays an important role in photochemical reactions. PAN is thought to contribute significantly to the global transport and distribution of reactive nitrogen as it can be transported over long distances in the free troposphere where low temperatures prevent its thermal decomposition, and it can return to the warmer, lower troposphere in remote areas where NO_2 is released from the thermal decomposition reaction and contributes to ozone formation [*Singh and Hanst*, 1981; *Cox and Roffey*, 1977; *Moxim et al.*, 1996].

[1]School of Environmental Science and Engineering, Sun Yat-sen University, Guangzhou, China.
[2]National Center for Atmospheric Research, Boulder, Colorado, USA.
[3]Air Quality Research Division, Science and Technology Branch, Environment Canada, Toronto, Ontario, Canada.
[4]School of Earth and Atmospheric Sciences, Georgia Institute of Technology, Atlanta, Georgia, USA.
[5]Purdue University, West Lafayette, Indiana, USA.
[6]Atmospheric Modeling and Analysis Division, U.S. Environmental Protection Agency, Research Triangle Park, North Carolina, USA.

0148-0227/12/2011JD016751

Deposition of PAN on surfaces provides another removal pathway through which the amount of reactive nitrogen within the surface layer is reduced and a source of atmospheric nitrogen is supplied to the ecosystem.

[4] *Sparks et al.* [2003], using a PAN concentration of 250 pptv in a chamber study, reported maximum dry deposition velocities (V_d) of PAN between 0.20–0.54 cm s^{-1} for eight plant species. The PAN uptake was found to be controlled by the stomatal pathway. In earlier field measurements, $V_d(PAN)$ was determined by some indirect techniques (e.g., the boundary layer budget technique, the gradient method). *Shepson et al.* [1992] measured $V_d(PAN)$ greater than 0.5 cm s^{-1} at night over a rural/agricultural area and two deciduous/coniferous forest sites. *Schrimpf et al.* [1996] determined $V_d(PAN)$ to be 0.54 ± 0.94 cm s^{-1} during nighttime above a corn field. *Doskey et al.* [2004] reported a small $V_d(PAN)$ of 0.13 ± 0.13 cm s^{-1} during the daytime at a grassland site and suggested that the stomatal uptake contributed mainly to the PAN flux while the contribution of thermal decomposition was less than 15%. Currently, the eddy covariance (EC) method is being used as a standard technique for flux measurements for energy, water vapor, CO_2, as well as air pollutants [*Ingwersen et al.*, 2011]. *Farmer et al.* [2006] conducted full annual cycle EC measurements of total peroxyacyl and peroxy nitrates (∑PNs) over a ponderosa pine canopy at the University of California Blodgett Forest Research Station. Downward fluxes were observed during wintertime, but the summertime measurements showed upward fluxes, probably due to a chemical flux divergence involving oxidation of NO_2 and acetaldehyde below the measurement height by elevated OH concentration within the canopy [*Farmer and Cohen*, 2008]. Recently, reliable fast response sensors for PAN have been developed and the EC fluxes of PAN to canopy were measured over two U.S. pine forests at Duke Forest, North Carolina [*Turnipseed et al.*, 2006] and at Blodgett Forest, California [*Wolfe et al.*, 2009]. Both data sets showed net downward PAN flux and similar diurnal trends that peaked around midday and remained at smaller values throughout the night. $V_d(PAN)$ at Duke Forest showed a daytime maximum of ~1 cm s^{-1} and typical nighttime values of 0.2–0.6 cm s^{-1}, which were much faster than predicted values by the Regional Acid Deposition Model (RADM). The deposition of PAN represented ~20% of the simultaneously measured daytime NO_y flux. At Blodgett Forest, the measured maximum $V_d(PAN)$ showed typical values of 0.4 cm s^{-1} and nighttime values were generally <0.2 cm s^{-1}. At Blodgett Forest, since there were strong vertical gradients in temperature due to surface heating, thermal decomposition was estimated to account for 31–65% of the measured PAN flux, and the portion varied significantly with temperature. *Wolfe and Thornton* [2011] developed a vertically resolved 1-D chemical transport model (CAFE) which had a fine vertical resolution of 0.1 m near the surface and described the details of turbulent diffusion, emission, deposition, and chemical reactions extending from the within canopy air space to the mixed layer. Modeled gradients of PAN concentrations were found to be in good agreement with the measurements, however the underprediction in the PAN flux and V_d reached above a factor of 2. This model-measurement disagreement was attributed to the underestimation of nonstomatal uptake, or uncertainties in gas phase chemistry and vertical mixing [*Wolfe et al.*, 2011].

[5] To date, the performance of $V_d(PAN)$ estimation by dry deposition models widely used in Chemistry and Transport Models (CTM) has not been systematically evaluated. Although the dry deposition process cannot compete with chemical losses because of thermal decomposition at typical daytime temperatures during the summer season, it could be a primary sink of PAN at night or during cold seasons [*Turnipseed et al.*, 2006]. It may also represent a significant source of atmospheric nitrogen to ecosystems that has thus far been ignored [*Sparks et al.*, 2003]. Therefore, $V_d(PAN)$ in CTMs must be treated as accurately as possible in order to predict PAN deposition and O_3 formation, especially for remote areas. It is imperative to assess the ability of dry deposition models to capture the variation in $V_d(PAN)$.

[6] The present study aims to evaluate the performance of two community dry deposition models in calculating $V_d(PAN)$, taking advantage of the newly available data of *Turnipseed et al.* [2006]. One model is the WRF-Chem dry deposition module [*Grell et al.*, 2005; *Wesely*, 1989] (hereinafter referred to as WDDM) and the other is the Noah land surface model (LSM) [*Chen and Dudhia*, 2001; *Ek et al.*, 2003] coupled with a photosynthesis-based Gas Exchange Model [*Niyogi et al.*, 2009; *Wu et al.*, 2011] (hereinafter referred to as Noah-GEM). We previously evaluated the performance of WDDM and Noah-GEM in simulating $V_d(O_3)$ and $V_d(NO_y)$ [*Wu et al.*, 2011] and found that a large WDDM measurement discrepancy was attributed to the minimum canopy stomatal resistance (R_i) based treatment of the canopy and Noah-GEM shows a better ability to capture the variations of canopy stomatal uptake than WDDM. In this paper, we coupled Noah-GEM with a more sophisticated nonstomatal resistance scheme [*Zhang et al.*, 2003] which is a function of u_*, *RH*, *LAI*, and canopy wetness for nonstomatal uptake, instead of the constant values used in WDDM. The measurement site, available data, and the two dry deposition models are briefly described in section 2. Model evaluation and sensitivity tests are described in detail in section 3. The summary of major conclusions and some recommendations are provided in section 4.

2. Methodology

2.1. Site Description

[7] The measurements were conducted at the Duke Forest FACE (Free Air CO_2 Enrichment) site at one of the control towers (i.e., no enhanced CO_2 levels). The site is in a 25 year old forest plantation of Loblolly pine (*Pinus taeda L.*) with a diversity of understory primarily of sweetgum (*Liquidambar styraciflua*), but also containing red maple (*Acer rubrum*), winged elm (*Ulmus alata Michx*), and flowering dogwood (*Cornus florida*) in North Carolina (35.98°N, 79.09°W; elevation, 163 m). The vegetation is fairly homogeneous within the distance of ~1 km in the direction of the dominant wind direction (southwest). The canopy height is on average ~17 m with a leaf area index (LAI) of 5.6 m^2 m^{-2} [*Palmroth et al.*, 2005].

[8] Measurements of 30 min average PAN fluxes and concentrations were taken at a height of 26 m between 16

and 25 July 2003 (day of year 197–206), accompanied with the associated meteorological data (i.e., air temperature, relative humidity, wind speed/direction, surface pressure, precipitation rate, and solar radiation). *Turnipseed et al.* [2006] reported that the average relative flux error on single flux measurements was ±41%. Although not reported in the previous paper, daytime values were typically smaller (25–35%). This large measurement uncertainty causes a large degree of scatter in the direct 30 min flux comparisons with the model. Therefore we also provided a comparison of simulated to observed diurnal averages, since this reduces the large run-to-run measurement variability. Further details on the site, instrumental methods, and uncertainty analysis can be found at http://c-h2oecology.env.duke.edu/site/main.html or in the work of *Turnipseed et al.* [2006].

2.2. Model Description and Configuration

[9] In existing single-layer (or big leaf type) deposition models, the dry deposition velocity (V_d) for a gaseous compound is determined as the reciprocal of a series of resistances to transport down to the surface [*Wesely and Hicks*, 2000]:

$$V_d(z) = (R_a(z) + R_b + R_c)^{-1}, \tag{1}$$

where R_a is the aerodynamic resistance, R_b the quasi-laminar sublayer resistance, R_c the surface resistance, and z the reference height.

[10] The conventional micrometeorological approaches based on similarity theory are used to estimate R_a and R_b in WDDM and Noah-GEM, as described by *Wu et al.* [2011], while the fundamental difference between WDDM and Noah-GEM exists in the R_c parameterization employed. The deposition may take place both through stomata and onto the exterior surface. R_c can then be generalized from both models as

$$\frac{1}{R_c} = \frac{1 - W_{st}}{R_s + R_m} + \frac{1}{R_{ns}}, \tag{2}$$

where R_s is the canopy stomatal resistance, R_m the mesophyll resistance, R_{ns} the resistance for uptakes by leaf cuticles, bark, soil, or ground litter, grouped together as nonstomatal, and W_{st} the fraction of stomatal blocking under wet conditions [*Zhang et al.*, 2003]. For WDDM, the effect of stomatal blocking is not considered and a value of 0 is given to W_{st}. Instead, dry and wet canopies were treated separately in this model. WDDM employs the R_c parameterization of *Wesely* [1989] that estimates R_s using a minimum canopy stomatal resistance (R_i) according to

$$R_s = R_i \left[1 + \left(\frac{200}{G + 0.1}\right)^2\right] \left[\frac{400}{T_s(40 - T_s)}\right] \tag{3}$$

where G is the solar irradiation and T_s the surface air temperature. In the work of *Wesely* [1989], R_{ns} is formulated as

$$\frac{1}{R_{ns}} = \frac{1}{R_{lu}} + \frac{1}{R_{dc} + R_{cl}} + \frac{1}{R_{ac} + R_{gs}}, \tag{4}$$

where R_{lu} is the leaf cuticle resistance, R_{dc} the resistance for buoyant convection in canopies, R_{cl} the resistance for leaves, twig, bark, or other exposed surfaces in the lower canopy, R_{ac} the in canopy aerodynamic resistance, and R_{gs} the ground or soil resistance. The R_{ns} components for SO_2 and O_3 are mainly derived from look-up tables, and then scaled for other gases based on their effective Henry's law constant (H^*) and reactivity factor (f_0). The readers are directed to the work of *Wesely* [1989] for a detailed description of all of these formulas and their parameters. Noah-GEM estimates R_s by considering the physiological process of the leaf response to net CO_2 assimilation/photosynthesis rate (A_n), the relative humidity fraction at the leaf surface (h_s), and CO_2 partial pressure at the leaf surface (C_s) [see *Ball et al.*, 1987; *Niyogi et al.*, 2009; *Wu et al.*, 2011]:

$$\frac{1}{R_s} = \left(m\frac{A_n h_s}{C_s}P + b\right) LAI, \tag{5}$$

where P is the atmospheric pressure and m and b are the slope and intercept obtained by linear regression analysis of data from gas exchange experiments. The R_{ns} calculated in Noah-GEM is parameterized according to *Zhang et al.* [2003]

$$\frac{1}{R_{ns}} = \frac{1}{R_{ac} + R_g} + \frac{1}{R_{cut}}, \tag{6}$$

where R_{ac} is the in canopy aerodynamic resistance which is common to all gases and R_g and R_{cut} are the resistances for the uptake by ground/soil and canopy cuticle. Similar to the work of *Wesely* [1989], R_g and R_{cut} are parameterized for SO_2 and O_3 and then scaled for other gases according to

$$\frac{1}{R_x(i)} = \frac{\alpha(i)}{R_x(SO_2)} + \frac{\beta(i)}{R_x(O_3)}, \tag{7}$$

where i represents the particular gas and parameters α and β are two scaling factors based on the chemical species' solubility and half-redox reactivity. *Zhang et al.* [2003] parameterized the nonstomatal resistances as a function of u_*, *RH*, *LAI*, and canopy wetness.

[11] Another difference between WDDM and Noah-GEM is the wetness definition. WDDM defines the surfaces to be wet either during precipitation events or when *RH* is >95%. Noah-GEM calculates the water content on the canopy surface (*CMC*) from the intercepted precipitation and dew formation [*Chen and Dudhia*, 2001] and then defines the surfaces to be wet when *CMC* is >0, which is more sophisticated compared with that in WDDM.

[12] The WDDM was extracted from the WRF-Chem model V3.1.1 and executed in a 1-D mode. The Noah LSM V3.1 (with GEM) was executed in the same fashion. The prescribed surface parameters were modified according to the site conditions (z_0 = 1.7 m, LAI = 5.6 m^2 m^{-2}). The 30 min interval measurements of air temperature (T), relative humidity (*RH*), wind speed (*WS*), wind direction (*WD*), atmospheric pressure (P_a), precipitation rate (P_{recip}), and downward shortwave radiation (R_{g_in}), gap filled by the data from the Duke Forest Loblolly Pine AmeriFlux site, were used to drive Noah-GEM. The forcing input of downward longwave radiation (R_{long_in}) was from the one-eighth degree hourly North American Land Data Assimilation System (NLDAS) outputs [*Mitchell et al.*, 2004; see also http://

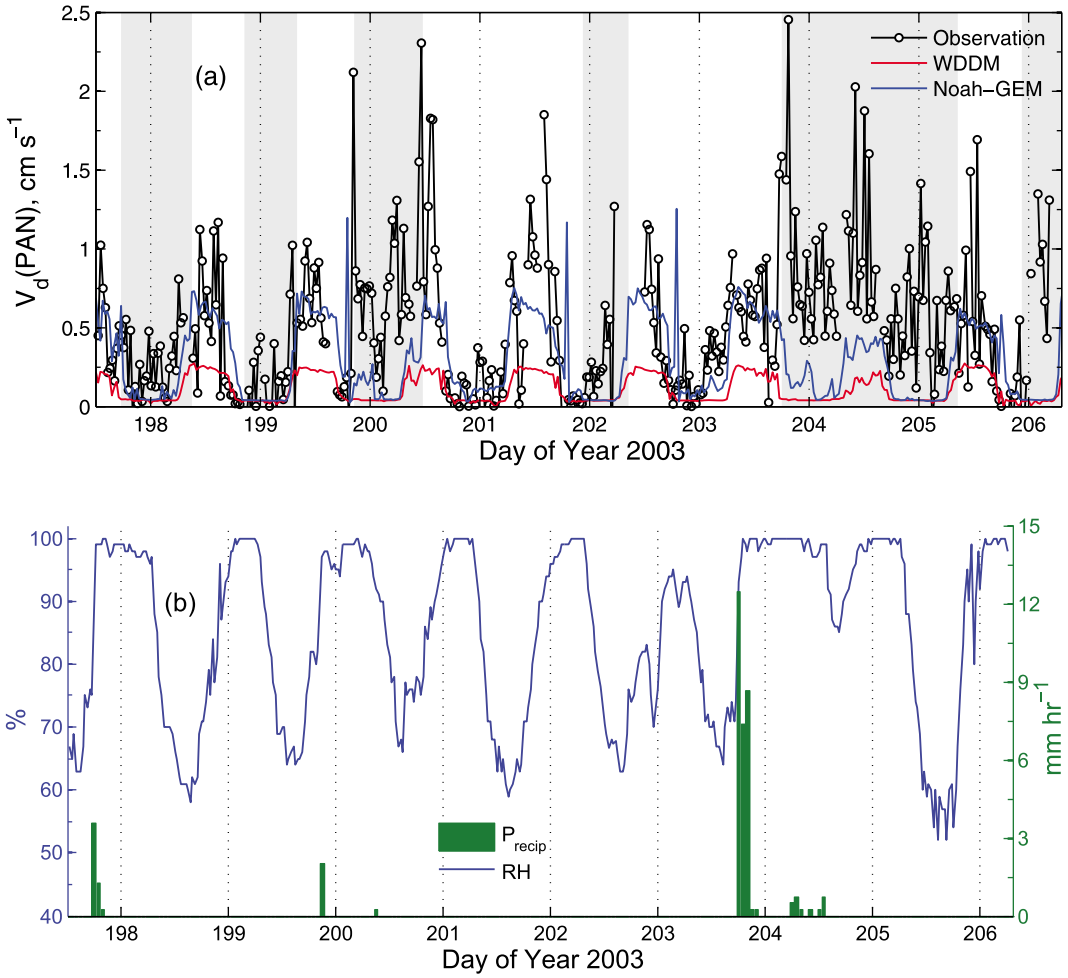

Figure 1. (a) Comparison of time series for observed and modeled $V_d(PAN)$. The shaded (white) boxes correspond to the wet (dry) surface conditions as determined from the water content on the canopy surface computed in the Noah land surface model coupled with a photosynthesis-based Gas Exchange Model (Noah-GEM). (b) Time series of observed relative humidity (RH) and precipitation (P_{recip}).

www.emc.ncep.noaa.gov/mmb/nldas/]. Noah simulated friction velocity (u_*) and Obukhov length (L) via a Monin-Obukhov similarity based iterative process, using air temperature, humidity, pressure, and wind speed [*Chen et al.*, 1997; *Chen and Zhang*, 2009]. WDDM requires inputs of T, R_{g_in}, RH, P_{recip}, u_* and L ($L = -\rho C_p u_*^3 \theta / kgH$) obtained from measurements.

3. Results and Discussion

3.1. Initial Model Performance

[13] Figure 1 compares simulated $V_d(PAN)$ by WDDM and Noah-GEM against the observations, with different boxes noting different surface conditions (dry or wet, determined by Noah-GEM). Table 1 presents the statistical results of the comparison.

[14] The observed $V_d(PAN)$ displayed large variations, but exhibited a diurnal pattern with peak values (on average) of ~1.0 cm s^{-1} at midday. Nocturnal $V_d(PAN)$ was small, but significantly different from zero with typical values ranging from 0.2 to 0.6 cm s^{-1}. There were several detectable precipitation events during the measurement period and the Duke Forest site was also quite humid (Figure 1b). Careful examination of the time series in Figure 1 reveals a clear tendency toward larger $V_d(PAN)$ under wet conditions because of rain or dew [see also *Turnipseed et al.*, 2006]. Also statistical results in Table 1 shows that the median $V_d(PAN)$ values at night(day) were 0.14 (0.53) and 0.43 (0.69) cm s^{-1} for dry and wet conditions, respectively, exhibiting significantly enhanced PAN uptake by the wet canopy surface. The increase of $V_d(PAN)$ because of wetness enhancement during the daytime was smaller than that during nighttime, which should be due to the offset effect of stomatal blocking under daytime wet conditions, similar to what was found for O_3 [*Zhang et al.*, 2002].

[15] WDDM predicted much smaller $V_d(PAN)$ compared to observations under all conditions (i.e., day or night, dry or wet) with a correlation coefficient of 0.32. $V_d(PAN)$ modeled by WDDM peaked at ~0.2 cm s^{-1} during noon and remained at a very low value of 0.04 cm s^{-1}, showing almost no differences between dry and wet conditions. Noah-GEM predicted larger $V_d(PAN)$ than WDDM, but still did not agree well with the observations, with a correlation coefficient of 0.24. During nighttime, $V_d(PAN)$ modeled by

Table 1. Statistical Results of Observed and Modeled $V_d(PAN)$ (cm s^{-1})[a]

	All (N = 349)			Day, Dry (N = 121)			Day, Wet (N = 30)			Night, Dry (N = 41)			Night, Wet (N = 108)		
	Ave	Med	R	Ave	Med	R	Ave	Med	R	Ave	Med	R	Ave	Med	R
Observation	0.54	0.47	–	0.59	0.53	–	0.93	0.69	–	0.17	0.14	–	0.50	0.43	–
WDDM	0.11	0.05	0.32	0.21	0.23	0.47	0.13	0.14	0.25	0.04	0.04	0.35	0.04	0.04	0.19
Noah-GEM	0.29	0.19	0.24	0.56	0.59	0.32	0.36	0.35	0.17	0.10	0.10	0.45	0.07	0.05	0.27
WDDM A1	0.24	0.05	0.31	0.52	0.57	0.48	0.31	0.33	0.27	0.04	0.04	0.35	0.04	0.04	0.19
WDDM A2	0.50	0.55	0.57	0.61	0.68	0.48	0.68	0.71	0.46	0.27	0.18	0.58	0.40	0.42	0.49
Noah-GEM S1	0.32	0.26	0.40	0.55	0.59	0.38	0.40	0.41	0.51	0.11	0.08	0.61	0.15	0.12	0.58
Noah-GEM S2	0.53	0.51	0.52	0.71	0.73	0.31	0.84	0.86	0.52	0.25	0.18	0.61	0.35	0.29	0.58

[a]Ave and Med are average and median values; N is the number of data samples; R is the correlation coefficient between observation and model simulation; Day is 08:00–18:00 (LST); Night is 20:00–05:00 (LST); "Dry" or "Wet" indicates the surface conditions as shown in Figure 1; A1 indicates that R_i was adjusted from the initial value of 130 s m^{-1} to 40 s m^{-1}; A2 indicates that R_i was adjusted from the initial value of 130 s m^{-1} to 40 s m^{-1} and R_{lu} of 650 s m^{-1} and 125 s m^{-1} were assigned for dry and wet surfaces, respectively; S1 indicates the measured u_* and L are used instead of that calculated by Noah-GEM; S2 indicated the measured u_* and L are used and the reactivity scaling factor β was adjusted from the initial value of 0.6 to 2.

Noah-GEM was larger and exhibited more variations than WDDM, more closely approaching the observations in terms of both magnitude and correlation. During the daytime, Noah-GEM underestimated $V_d(PAN)$ around noontime and overestimated $V_d(PAN)$ in the afternoon, resulting in relatively low correlations (R = 0.17–0.32). *Wu et al.* [2011] also found Noah-GEM tended to overestimate $V_d(O_3)$ in the afternoon, which was explained by the lack of considering the accumulation effect of stomatal fluxes on plant leaf uptake in the model. Other possible reasons include that the stress function currently being used for soil moisture interaction or the coupling coefficient being used are insufficient [*Chen and Zhang*, 2009; *Charusombat et al.*, 2012] and will need to be modified in future work.

[16] As previously discussed, WDDM and Noah-GEM employ different R_s and R_{ns} schemes. Figure 2 shows that there were large differences between WDDM and Noah-GEM in estimating R_s and R_{ns}. WDDM simulated a nearly constant R_{ns} of ~2400 s m^{-1}, while R_{ns} simulated by Noah-GEM exhibited a significant diurnal trend with smaller values during the daytime (~500 s m^{-1}) and larger values at night (~1500 s m^{-1}). Diurnal profiles in R_s were similar as the R_s schemes in both models assumed complete stomatal closure at dark. However, Noah-GEM predicted R_s of ~250 s m^{-1} at noon, only half of that modeled by WDDM.

[17] At night, stomatal uptake and thermal decomposition are all suppressed because of stomatal closure, larger NO_2/NO ratios, and lower temperature. The nonstomatal uptake to other surfaces, including leaf cuticles, bark, soil, or ground litter should be considered as the only pathway for PAN decay. So R_{ns} equals R_c at night. As in the work of *Zhang et al.* [2002], we determined the observed R_c according to

$$R_c = V_d{}^{-1} - R_a - R_b, \tag{8}$$

where R_a and R_b were calculated in WDDM using measured meteorological variables (i.e., u_* and L), and the observed V_d were used in equation (8). We derived the observed R_{ns} at night by only using the nighttime data. We then divided the whole data into data sets under dry and wet conditions which was determined from the water content on the canopy surface computed in Noah-GEM (see section 2.2 and Figure 1). The median R_{ns} was calculated to be 650 s m^{-1} under dry conditions and decreased to 125 s m^{-1} under wet conditions, much smaller than the estimates by WDDM (~2400 s m^{-1}) and Noah-GEM (~1500 s m^{-1}). Mean R_{ns} values are strongly influenced by a small number of extreme large data points. *Turnipseed et al.* [2006] adopted a similar approach and suggested 244 s m^{-1} when dry and 125 s m^{-1} when wet. The main difference in calculating the R_{ns} between this study and the work by *Turnipseed et al.* [2006] is the definition of wetness. In the work of *Turnipseed et al.* [2006], an oversimplified definition of wetness similar to WDDM was used where the surface is defined to be wet either during and immediately following precipitation events or when ambient RH was >96%. The data subset under dry conditions obtained using that wetness definition should include some time points with residual precipitation on the canopy surface which was divided into the wet period in this study, and thus had a larger average V_d and lower R_{ns}.

[18] Because direct measurements of R_s were not available at the Duke Forest site, examining the observed surface heat fluxes against the model outputs provided an independent assessment of R_s (surface heat fluxes are the primary outcomes for LSMs such as Noah-GEM, but are not provided by WDDM). Figure 3 shows that Noah-GEM–modeled heat fluxes are in good agreement with measurements, thereby

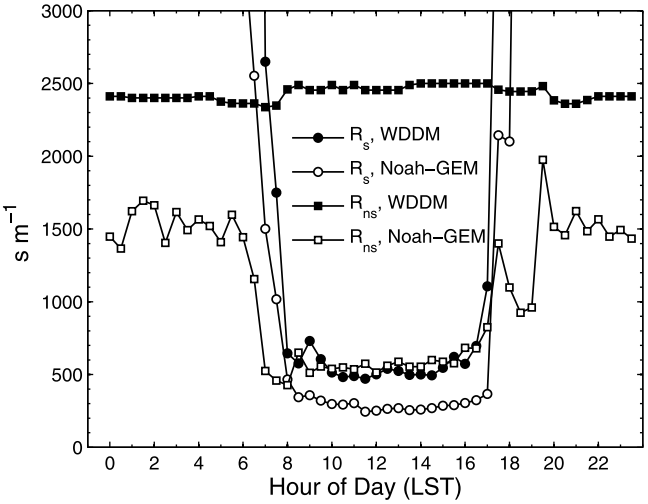

Figure 2. Average diurnal cycles of stomatal resistance (R_s) and nonstomatal resistances (R_{ns}) for peroxyacetyl nitrate (PAN) modeled by WRF-Chem dry deposition module (WDDM) and Noah-GEM.

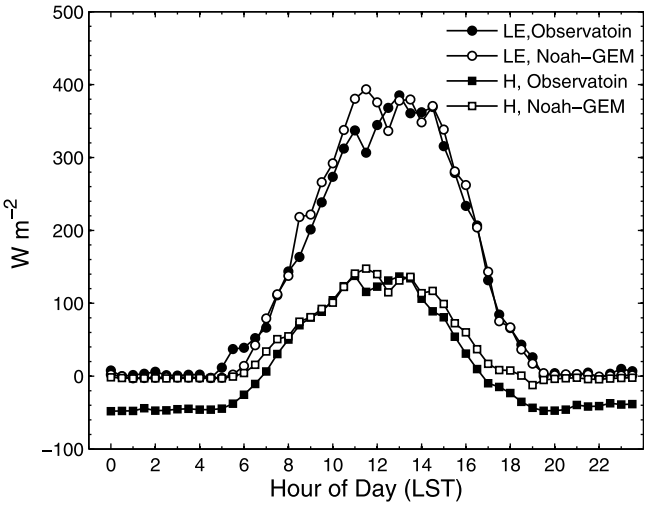

Figure 3. Comparison of observed and Noah-GEM–modeled average diurnal variations of latent heat flux (*LE*) and sensible heat flux (*H*).

demonstrating some confidence in the simulation of R_s by Noah-GEM, which in turn illustrates that WDDM overestimated R_s, by almost a factor of 2.

3.2. Chemical Influence on V_d(PAN)

[19] The measured flux of PAN to the canopy can be contributed by surface uptake (deposition) as well as air space chemical reactions below the sensor height [*Doskey et al.*, 2004; *Turnipseed et al.*, 2006; *Wolfe et al.*, 2009].

[20] The PA radical generated from the thermal decomposition of PAN (reaction (R2r)) can also deposit on the surface, potentially contributing to an observed downward flux of PAN. As the PA radical is one of the most powerful oxidants among the peroxy radicals [*Schuchmann and von Sonntag*, 1988] and the measurements [*Villalta et al.*, 1996; *Roberts et al.*, 1996] demonstrated that the heterogeneous hydrolysis could be a very efficient loss process for PA on an aqueous surface, we would expect a fast surface uptake of PA under both dry and wet conditions. *Wolfe et al.* [2009] estimated the contribution of PA deposition to PAN flux in the Blodgett Forest case and found the fraction was <5% even when considering the surface as a perfect sink for PA, i.e., the maximum V_d of PA ($V_{max} = (R_a + R_b)^{-1}$) was given. The small fraction was mainly attributed to the much lower PA concentrations compared with PAN. *Turnipseed et al.* [2006] also suggested a negligible influence of PA surface deposition on PAN flux in the Duke Forest case from the viewpoint of time scales since the calculated rate of PAN thermal decomposition is much slower than the rate of turbulent diffusion.

[21] Both *Doskey et al.* [2004] and *Wolfe et al.* [2009] showed evidence that within the atmospheric surface layer, thermal decomposition of PAN (reaction (R2r)) and subsequent loss via reaction (R3) can contribute to the measured above canopy flux when the thermal decomposition rate varies significantly with altitude below the flux measurement height. Although this also depends on the gradient of the chemical partitioning between NO and NO_2, *Wolfe et al.* [2009] showed that the change in the decomposition rate was the major contributing factor. If a large temperature gradient due to strong daytime surface heating is present, the equilibrium of reaction (R2) shifts toward PA and NO_2 in the region closer to the surface, which can lead to a gradient in PAN concentrations and, thus, a downward flux of PAN (as was the case in the study of *Wolfe et al.* [2009]).

[22] Reliable absolute temperature gradient measurements (as well as chemical gradients of [NO]/[NO_2]) were not

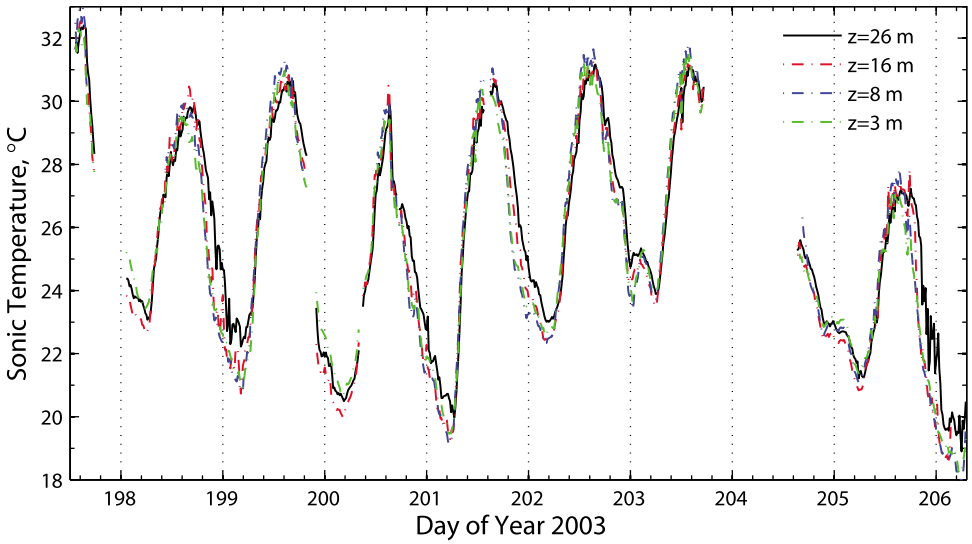

Figure 4. Air temperatures measured by the sonic anemometer at the height of 3, 8, 16, and 26 m above the surface (3, 8, and 16 m were at the bottom, middle, and top of the canopy, respectively; 26 m was the flux measurement height). Data has been removed for the hours during and immediately following precipitation events. For median midday mixing ratios of [NO] = 198 pptv and [NO_2] = 1666 pptv, the thermal lifetime for PAN is estimated to be 1.1 h at 32°C; for median midnight mixing ratios of [NO] = 91 pptv and [NO_2] = 1662 pptv, the thermal lifetime for PAN is estimated to be 12.3 h at 20°C.

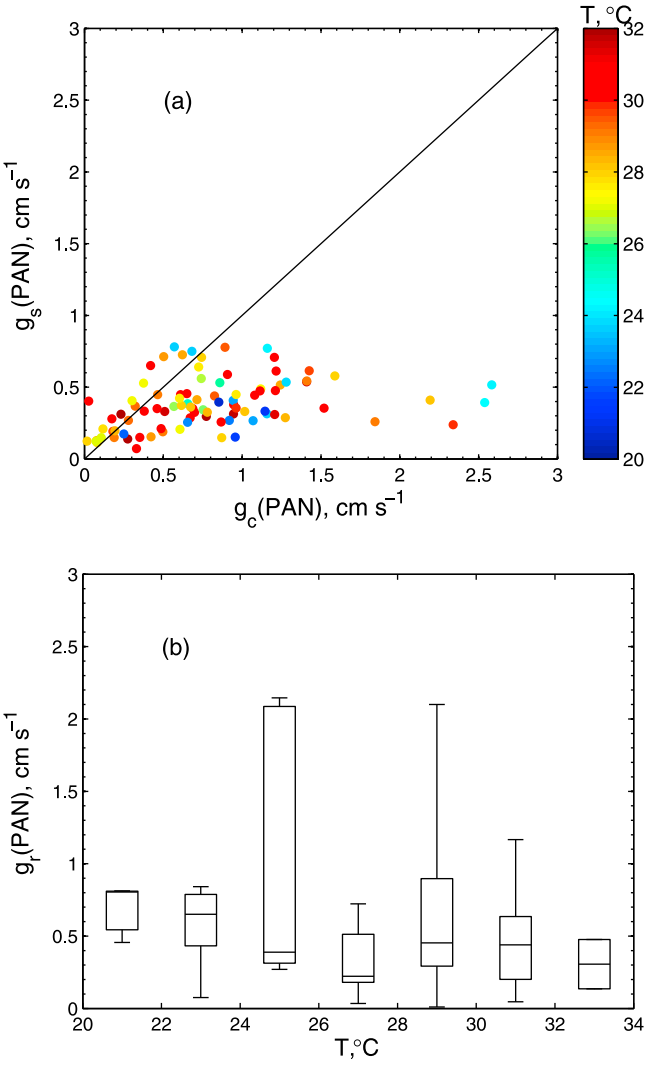

Figure 5. (a) Scatterplot of canopy stomatal conductance for PAN ($g_s(PAN)$) versus surface conductance for PAN ($g_c(PAN)$), color-mapped by air temperature. Only points during 08:00–18:00 (LST) are shown, and data has been removed when precipitation was measured. The line drawn is the 1:1 line. (b) Whisker box plot of the residual conductance ($g_r(PAN) = g_c(PAN) - g_s(PAN)$) for 2°C intervals of the air temperature. On each box, the central mark is the median, the edges of the box are the 25th and 75th percentiles, and the whiskers extend to the extreme data points. The g_s was calculated using the inversion of the Penman-Monteith equation; g_c was determined as $(V_d(PAN)^{-1} - R_a - R_b)^{-1}$. Further details are provided by *Turnipseed et al.* [2006].

available during the Duke Forest campaign; however, temperatures derived from a vertical profile of sonic anemometers (at z = 3, 8, 16, and 26 m) showed the expected pattern of a warmer daytime canopy and colder temperatures within the canopy at night (Figure 4). Although the uncertainty of these gradients is likely substantial, this data suggested that midday temperature gradients were typically <1°C (often only around 0.5°C). Further evidence to support small temperature gradients comes from the observations that latent heat fluxes were typically twice as large as sensible heat fluxes (Figure 3), indicating that energy partitioning in this ecosystem strongly favored water evaporation over sensible heating of the air. *Wolfe et al.* [2009] observed that higher values of surface conductance ($g_c(PAN)$) were associated with increased temperatures. Reevaluating the data set of *Turnipseed et al.* [2006], we do not see such a dependence (compare our Figure 5a with Figure 8 of *Wolfe et al.* [2009]). Figure 5b shows the variation of the residual conductance ($g_r(PAN) = g_c(PAN) - g_s(PAN)$) with increasing temperature. There was no increase of $g_r(PAN)$ with increasing temperature, suggesting that thermal decomposition was relatively unimportant for the observed PAN fluxes during this study. However, as shown by *Wolfe et al.* [2009] and *Doskey et al.* [2004], the thermal decomposition effect was an important contributing factor during periods of strong sensible heat flux and must be considered when comparing with deposition models.

3.3. Sensitivity Tests and Model Improvements

3.3.1. WDDM

3.3.1.1. Stomatal Pathway (R_s)

[23] WDDM estimates R_s based on the prescribed minimum canopy stomatal resistance (R_i) (equation (3)). Many studies [e.g., *Cooter and Schwede*, 2000; *Wu et al.*, 2011] have shown that uncertainty in the prescribed R_i can dominate the errors in estimating R_s and thus V_d of the gases controlled by stomatal pathways. Here, we conducted sensitivity tests, differing only by the value of R_i in WDDM and compared the R_s output with that calculated from Noah-GEM as it was evaluated by comparing against observations of water vapor exchange. We found that R_i of 40 s m^{-1} instead of the initial value of 130 s m^{-1} [see *Wesely*, 1989] generated values of R_s close to Noah-GEM. The modeled daytime $V_d(PAN)$ by WDDM increased by more than a factor of two, more closely approaching the observations (Table 1 and Figure 6a). The correlations did not improve significantly, however, suggesting that some key factors could not be captured by the model if only modifying R_i.

[24] Although reducing R_i (from 130 to 40 s m^{-1}) improved the model performance (on averaged V_d, but not on the correlation between model and measurement) for this site, the reduced value might not be suitable for different forest sites. The real reason for the poor performance of WDDM is that the simple formula for R_s (equation (3)) does not consider factors dominating stomatal resistance, such as the canopy biological information (e.g., *LAI*) as well as some environmental stress functions (e.g., vapor pressure deficit, and soil moisture) which are essential in order to obtain adaptable R_s prediction over different vegetated surfaces and regions. Many stomatal resistance submodules following the more sophisticated Jarvis style empirical equation are available [e.g., *Baldocchi et al.*, 1987; *Hicks et al.*, 1987; *Meyers et al.*, 1998; *Zhang et al.*, 2001]. Photosynthesis-based semiempirical equations have also been developed for estimating stomatal uptake [e.g., *Niyogi et al.*, 2009; *Wu et al.*, 2003; *Hirabayashi et al.*, 2011]. A comparison between these two types of stomatal equations by *Niyogi and Raman* [1997] found that the photosynthesis-based equation is more responsive to the external environmental conditions and thus consistently performs better in simulating R_s than the Jarvis style equation.

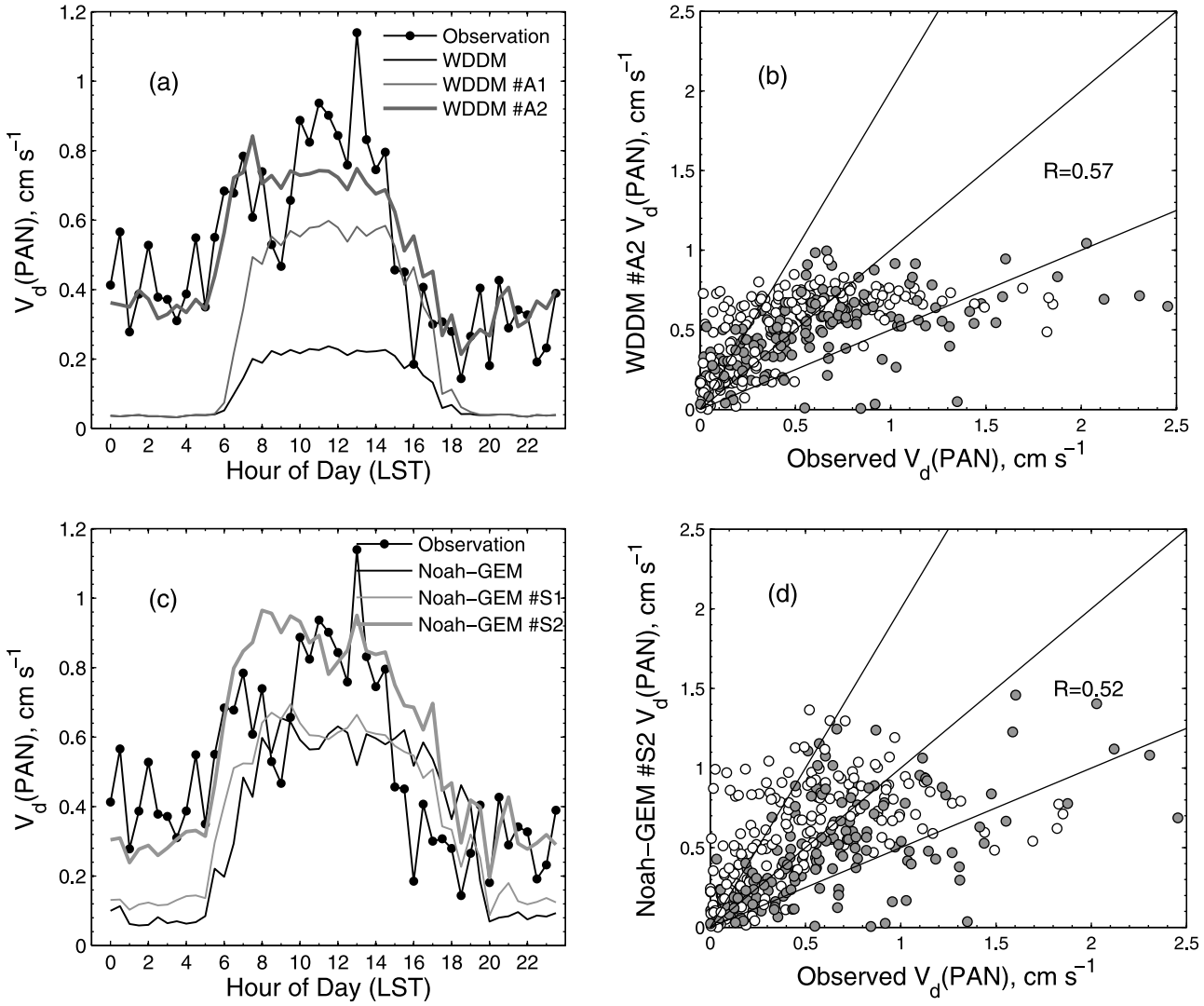

Figure 6. (a) Comparison of observed and WDDM-modeled average diurnal cycles of $V_d(PAN)$. (b) Scatterplots of observed and WDDM-modeled $V_d(PAN)$. (c) Same as Figure 6a but for Noah-GEM. (d) Same as Figure 6b but for Noah-GEM. The shaded (white) cycles correspond to the wet (dry) surface conditions; A1, A2, S1, and S2 are shown as in Table 1; the lines drawn are the 2:1, 1:1, and 1:2 lines, respectively.

3.3.1.2. Nonstomatal Pathway (R_{ns})

[25] WDDM simply parameterizes the R_{ns} components based on specified constant values, which minimizes the complexity and computational cost. Here we replaced the constant values with those derived from observations (see section 3.1). *Turnipseed et al.* [2006] suggested that because of the low within canopy transport in the stable conditions of night (the transfer resistance within the canopy were greater than 2000 s m^{-1} in the models), the primary loss pathway at night was most likely via cuticular deposition over the upper canopy. Therefore we assigned 650 s m^{-1} when wet and 125 s m^{-1} when dry to cuticular resistance (R_{lu}) in WDDM and tested its influence on $V_d(PAN)$ estimates (WDDM A2). One limitation for this sensitivity test is that we also applied those values derived from nighttime measurements to daytime simulations. The R_{lu} during daytime may be different from that during nighttime, but the difference is expected to be relatively small [*Zhang et al.*, 2002].

[26] Table 1 shows that WDDM A2 modeled a very close $V_d(PAN)$ to the observation at night and the correlation also increased significantly. The adjustment of R_{lu} also improved the daytime simulation as the bias was reduced and the correlation increased. Figure 7 shows that WDDM A2 was in much better agreement with observations than the initial model results capturing the shape and magnitude of the observations. The simulated $V_d(PAN)$ by WDDM A2 was usually below 1.0 cm s^{-1}, however, around noon on most days, very high V_d values (i.e., >1.0 cm s^{-1}) were observed. Therefore the averaged diurnal curves (Figure 6a) show that WDDM A2 still underestimated the noon peak of $V_d(PAN)$, but when looking at the median values, the model was much closer to the observations (Table 1). Approximately 66% of

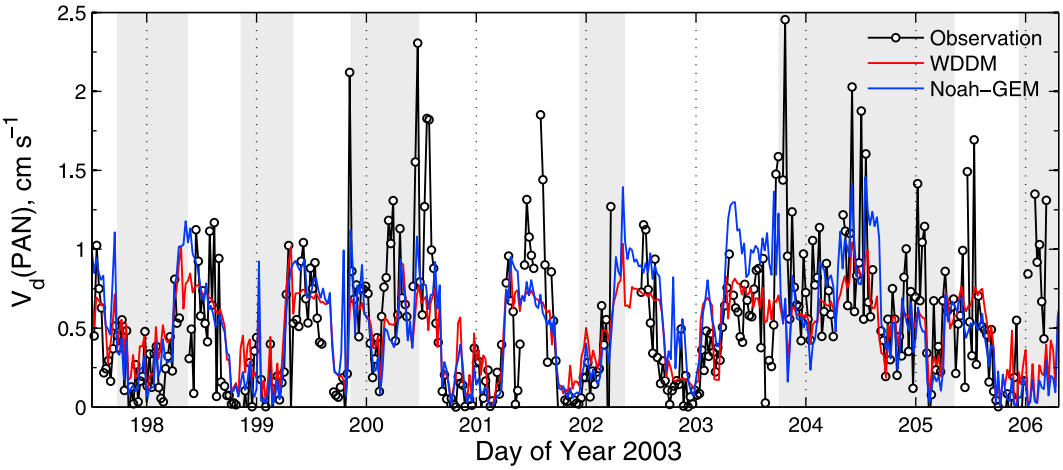

Figure 7. Comparison of time series of observed and modeled $V_d(PAN)$. The shaded (white) boxes correspond to the wet (dry) surface conditions; A2 and S2 are shown as in Table 1.

the WDDM A2 estimates are within a factor of 2 of the observed values (Figure 6b).

3.3.2. Noah-GEM

3.3.2.1. Atmospheric Resistances (R_a and R_b)

[27] The standard Noah-GEM model requires the input of routinely available meteorological variables (see section 2) but calculates some micrometeorological variables (e.g., u_* and L) itself via a Monin-Obukhov similarity based iterative process, using air temperature, humidity, pressure, and wind speed [*Chen et al.*, 1997; *Chen and Zhang*, 2009]. Figure 8 shows that Noah-GEM generally reproduced the magnitude and shape of observed u_*, but a large discrepancy can be observed especially during nocturnal stable conditions. In Noah-GEM, R_a, R_b and R_{ns} are dependent on u_* or L. Figure 6c shows that Noah-GEM modeled a slightly larger $V_d(PAN)$ if the measured u_* or L were used to calculate the resistances instead of that modeled by Noah-GEM. Statistical results (Table 1) reveal that the correlations improved significantly in every condition (day or night, dry or wet). The correlation coefficient for all the data increased from 0.24 to 0.40, implying that Noah-GEM captured a much better variation of the observed $V_d(PAN)$ because of improved inputs of u_* and L. The sensitivity of Noah-GEM V_d estimates to errors in meteorological inputs as well as model parameters will be evaluated systematically in future work.

[28] WDDM and Noah-GEM S1 were driven by the same set of u_*, L, and other standard meteorological variables without any tuning of the model parameters. Table 1 shows that Noah-GEM S1 modeled nocturnal $V_d(PAN)$ closer to the observations than WDDM, and the correlation for Noah-GEM S1 (R = 0.58–0.61) during nighttime was significantly higher than that for WDDM (R = 0.19–0.35). *Zhang et al.* [2003] has the explicit dependence of R_{ns} on the meteorological (u_* and RH), biological (LAI), and surface (canopy wetness) conditions and the results in this study suggest it is thus superior to the approaches simply using constant values. Future work to improve the model will involve assimilating more environmental factors (e.g., pH of soil and canopy surface water) and leaf scale processes (e.g., lipid dissolving into cuticle membrane, enzymatic conversion

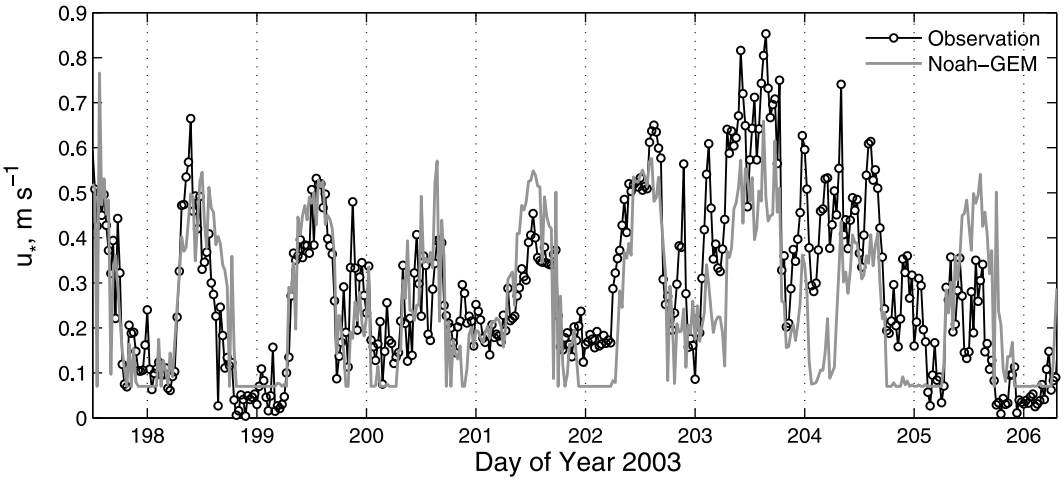

Figure 8. Comparison of time series of observed and Noah-GEM–modeled friction velocity (u_*).

within leaf interior [*Karl et al.*, 2010]) that essentially affect the canopy uptake of various pollutants.

3.3.2.2. Nonstomatal Pathway (R_{ns})

[29] As PAN has high oxidizing capacity and relatively limited solubility, the dry deposition of PAN was assumed to be similar to that of O_3 and the solubility scaling factor α and the reactivity scaling factor β (equation (7)) were specified to be 0 and 0.6, respectively, in Noah-GEM [*Zhang et al.*, 2003]. A few studies that simultaneously measured the uptakes of PAN and O_3 by vegetation during daytime or nighttime are available [*Hill*, 1971; *Garland and Penkett*, 1976; *Shepson et al.*, 1992; *Wolfe et al.*, 2009], but since the daytime fluxes can be influenced by chemical reactions as well as stomatal uptake, the nighttime results are more appropriate for comparing R_{ns} between PAN and O_3. There have previously been two studies that simultaneously measured the deposition of PAN and O_3 over vegetative area at night. *Shepson et al.* [1992] obtained average $V_d(PAN)/V_d(O_3)$ of 2.4 over three vegetative rural sites by measuring the nighttime concentration losses of PAN and O_3 and relating them to deposition, namely the boundary layer budget technique. EC fluxes of PAN and O_3 measured at Blodgett Forest by *Wolfe et al.* [2009] indicated $V_d(PAN)/V_d(O_3)$ of 0.50 at night. Thus these two studies indicate that the ratio $V_d(PAN)/V_d(O_3)$ ranges from 0.50 to 2.4 at night. Model estimates of this ratio by Noah-GEM S1 was from 0.60 to 1.0 with a median of 0.68, close to the results of *Wolfe et al.* [2009].

[30] We conducted the sensitivity tests by tuning the reactivity scaling factor β in Noah-GEM. The results show that increasing β can reduce the bias and enhance the correlation between observations and simulations by Noah-GEM. A value of 2 for β is found a better fit at this specific site. Also note that in Noah-GEM a decrease in cuticular resistance of PAN when the canopy was wet was assumed, which in fact resulted from the assumption of enhanced O_3 cuticle uptake by wet canopy in the model [*Zhang et al.*, 2002, 2003] and is consistent with field measurements [*Turnipseed et al.*, 2006]. As shown in Figure 7, with the adjustment of the β parameter from the initial value of 0.6 to 2, Noah-GEM was in much better agreement with the observations than the initial model results. The shape and magnitude of the observations was reproduced well except for a few very high observed V_d values >1.3 cm s^{-1}. However, the average diurnal cycles (Figure 6c) show that the model did not capture the midmorning decrease in the observed $V_d(PAN)$ and overestimated $V_d(PAN)$ in the afternoon. Approximately 68% of the Noah-GEM S2 estimates are within a factor of 2 of the observed values (Figure 6d). The ratio $V_d(PAN)/V_d(O_3)$ during nighttime modeled by Noah-GEM S2 ranged from 1.0 to 1.8 with a median of 1.6 which was in the middle of the range determined in field (0.50–2.4). Thus increasing β to the value of 2 still keeps the model outcomes consistent with the field observations. Recently the Community Multiscale Air Quality model (CMAQ) also increased its surface reactivity scaling parameter for PAN to obtain a larger $V_d(PAN)$ prediction based on the findings from recent measurements [*Pleim and Ran*, 2011]. However, generalization of this assumption is cautioned before measurement data are available over various canopies. It is very likely that the relative magnitude of $V_d(\mathrm{PAN})/V_d(\mathrm{O_3})$ and thus the β value varies under different conditions because of the chemical processes involved in the dry deposition processes.

4. Conclusions and Recommendations

[31] Modeled dry deposition velocities for PAN from two community dry deposition models, WDDM and Noah-GEM, were evaluated using eddy covariance flux measurements over a coniferous forest canopy. Both models underestimated $V_d(PAN)$ by a factor of 2–5 and the correlations between the model results and measurements were also very low, e.g., R = 0.32 and 0.24 for WDDM and Noah-GEM, respectively. The underprediction of the modeled V_d was largely attributed to the modeled stomatal and nonstomatal uptake since the influence of PAN thermal decomposition on measured fluxes was small.

[32] Through the adjustments of the model parameter or variable, WDDM and Noah-GEM can finally reach a satisfactory performance. However, a large challenge still exists for modeling $V_d(PAN)$ as our knowledge of the dry deposition process of PAN is still limited and the current adjustments would be considered more of an empirical fit to observations.

[33] Noah-GEM estimated more realistic stomatal uptake than WDDM (in terms of the average V_d values, but not the correlation) as was shown by a comparison with measured water vapor fluxes. This is because the former included the physiological process including the CO_2 assimilation rate while the latter used a prescribed minimum stomatal resistance without key biological factors (e.g., *LAI*). The newly adopted nonstomatal resistance parameterization in Noah-GEM also had a better capacity to capture the variations in $V_d(PAN)$, because of its dependence on biological (*LAI*), meteorological (u_*, *RH*), and surface (canopy wetness) conditions, than the simple R_{ns} parameterization in WDDM. This was demonstrated by the better modeled average V_d and better correlations from Noah-GEM than from WDDM using nighttime data only (when nonstomatal uptake dominates). The correlation between Noah-GEM–modeled V_d and measurements was also improved if using observed u_* and L instead of model calculated values, implying the importance of meteorological variables on the dry deposition processes.

[34] On the basis of sensitivity tests conducted in the present study and our current understanding of dry deposition processes, the following recommendations are provided for dry deposition modeling approaches suitable for use in chemical transport models. The stomatal uptake of PAN and many other gaseous pollutant species should be modeled using stomatal resistance submodules that at least consider key biological and meteorological variables that are available as input parameters to host models. As an example, the sunlit/shade stomatal resistance modules provide results as good as multilayer stomatal resistance modules but require less computer resources and fewer input parameters and are much more accurate than single-leaf modules [e.g., *De Pury and Farquhar*, 1997; *Zhang et al.*, 2001]. Further study is needed for the comparison of more sophisticated Jarvis type stomatal resistance modules with photosynthesis approach–based modules to help the community choose proper stomatal uptake modules.

[35] Nonstomatal uptake contributes ~50% of total dry deposition fluxes for PAN, O_3, and many other species and

need to be modeled more accurately. Most nonstomatal resistance parameterizations currently used in chemical transport models are very simple and require further evaluation and improvement. Many recent studies confirmed the strong dependence of the nonstomatal uptake on meteorological conditions, especially the friction velocity and canopy wetness. Thus, it is recommended that nonstomatal uptake include key meteorological and biological factors. High-quality dry deposition flux measurement data for PAN and other lesser understood species over various canopies are also needed in order to improve the nonstomatal resistance modules.

[36] Leaf area index is a key parameter for both stomatal and nonstomatal uptake; high temporal and spatial resolution data for LAI from remote sensing should be used as input for dry deposition modules within chemical transport models. Consistence of input parameters and/or meteorological variables (e.g., roughness length, soil moisture, canopy wetness, and many boundary layer micrometeorological variables) between the dry deposition module and its host model is preferred.

[37] The implementation of Noah-GEM calculated V_d in the WRF-Chem model is underway. This work is a first step and preliminary study to evaluate the dry deposition of nitrogen-bearing compounds which are critical for estimating the surface and atmospheric nitrogen budget in atmospheric chemistry models. Further evaluations using measurements over various sites and covering longer time periods are needed to better understand the dry deposition of PAN and narrow the uncertainties in model parameters.

[38] **Acknowledgments.** This work was supported in part by the following grants: the Natural Science Foundation of China (grants 40875076 and U0833001), the National Program on Key Basic Research Project of China (973) (grant 2010CB428504), the Fundamental Research Funds for the Central Universities, the National Center for Atmospheric Research (NCAR) Advanced Study Program (ASP), the NCAR BEACHON (Bio-hydro-atmosphere interactions of Energy, Aerosols, Carbon, H_2O, and Organics and Nitrogen) Program, the NCAR Water System Program, and the U.S. NSF DRInet (OCI and Hydrology). NCAR is operated by the University Corporation for Atmospheric Research (UCAR) under the sponsorship of the National Science Foundation (NSF). The authors thank the Duke FACE site and its staff for allowing us to work at their research site as well as the invaluable assistance they provided during this experiment. We would also like to thank Gabriel Katul and Paul Stoy for their permission to use data from the Duke Forest AmeriFlux data archives.

References

Baldocchi, D. D., B. B. Hicks, and P. Camara (1987), A canopy stomatal resistance model for gaseous deposition to vegetated surfaces, *Atmos. Environ.*, *21*, 91–101, doi:10.1016/0004-6981(87)90274-5.

Ball, J., I. Woodrow, and J. A. Berry (1987), A model predicting stomatal conductance and its contribution to the control of photosynthesis under different environmental conditions, in *Progress in Photosynthesis Research*, edited by J. Biggins, pp. 221–224, Nijhoff, Dordrecht, Netherlands.

Charusombat, U., D. Niyogi, S. Garrigues, A. Olioso, O. Marloie, M. Barlage, F. Chen, M. Ek, X. M. Wang, and Z. Y. Wu (2012), Noah-GEM and Land Data Assimilation System (LDAS) based downscaling of global reanalysis surface fields: Evaluations using observations from a CarboEurope agricultural site, *Comput. Electron. Agric.*, doi:10.1016/j.compag.2011.12.001, in press.

Chen, F., and J. Dudhia (2001), Coupling an advanced land surface–hydrology model with the Penn State–NCAR MM5 modeling system. Part I: Model implementation and sensitivity, *Mon. Weather Rev.*, *129*(4), 569–585, doi:10.1175/1520-0493(2001)129<0569:CAALSH>2.0.CO;2.

Chen, F., and Y. Zhang (2009), On the coupling strength between the land surface and the atmosphere: From viewpoint of surface exchange coefficients, *Geophys. Res. Lett.*, *36*, L10404, doi:10.1029/2009GL037980.

Chen, F., Z. Janjic, and K. Mitchell (1997), Impact of atmospheric surface-layer parameterization in the new land-surface scheme of the NCEP mesoscale Eta model, *Boundary Layer Meteorol.*, *85*, 391–421.

Cooter, E. J., and D. B. Schwede (2000), Sensitivity of the National Oceanic and Atmospheric Administration multilayer model to instrument error and parameterization uncertainty, *J. Geophys. Res.*, *105*(D5), 6695–6707, doi:10.1029/1999JD901080.

Cox, R. A., and M. J. Roffey (1977), Thermal decomposition of peroxyacetylnitrate in the presence of nitric oxide, *Environ. Sci. Technol.*, *11*(9), 900–906, doi:10.1021/es60132a010.

De Pury, D. G. G., and G. D. Farquhar (1997), Simple scaling of photosynthesis from leaves to canopies without the errors of big-leaf models, *Plant Cell Environ.*, *20*, 537–557, doi:10.1111/j.1365-3040.1997.00094.x.

Doskey, P. V., V. R. Kotamarthi, Y. Fukui, D. R. Cook, F. W. Breitbeil III, and M. L. Wesely (2004), Air-surface exchange of peroxyacetyl nitrate at a grassland site, *J. Geophys. Res.*, *109*, D10310, doi:10.1029/2004JD004533.

Ek, M. B., K. E. Mitchell, Y. Lin, E. Rogers, P. Grunmann, V. Koren, G. Gayno, and J. D. Tarpley (2003), Implementation of Noah land surface model advances in the National Centers for Environmental Prediction operational mesoscale Eta model, *J. Geophys. Res.*, *108*(D22), 8851, doi:10.1029/2002JD003296.

Farmer, D. K., and R. C. Cohen (2008), Observations of HNO_3, $\sum$AN, $\sum$PN and NO_2 fluxes: Evidence for rapid HO_x chemistry within a pine forest canopy, *Atmos. Chem. Phys.*, *8*, 3899–3917, doi:10.5194/acp-8-3899-2008.

Farmer, D. K., P. J. Wooldridge, and R. C. Cohen (2006), Application of thermal-dissociation laser induced fluorescence (TD-LIF) to measurement of HNO_3, $\sum$alkyl nitrates, $\sum$peroxy nitrates, and NO_2 fluxes using eddy covariance, *Atmos. Chem. Phys.*, *6*, 3471–3486, doi:10.5194/acp-6-3471-2006.

Garland, J. A., and S. A. Penkett (1976), Absorption of peroxy acetyl nitrate and ozone by natural surfaces, *Atmos. Environ.*, *10*, 1127–1131, doi:10.1016/0004-6981(76)90122-0.

Grell, G. A., S. E. Peckham, R. Schmitz, and S. A. Mceen (2005), Fully coupled "online" chemistry within the WRF model: Description and application, *Atmos. Environ.*, *39*, 6957–6975, doi:10.1016/j.atmosenv.2005.04.027.

Hicks, B. B., D. D. Baldocchi, T. P. Meyers, R. P. Hosker, and D. R. Matt (1987), A preliminary multiple resistance routine for deriving dry deposition velocities from measured quantities, *Water Air Soil Pollut.*, *36*, 311–330, doi:10.1007/BF00229675.

Hill, A. C. (1971), Vegetation: A sink for atmospheric pollutants, *J. Air Pollut. Control Assoc.*, *21*, 341–346.

Hirabayashi, S., C. N. Kroll, and D. J. Nowak (2011), Component-based development and sensitivity analyses of an air pollutant dry deposition model, *Environ. Modell. Software.*, *26*, 804–816, doi:10.1016/j.envsoft.2010.11.007.

Ingwersen, J., et al. (2011), Comparison of Noah simulations with eddy covariance and soil water measurements at a winter wheat stand, *Agric. For. Meteorol.*, *151*, 345–355, doi:10.1016/j.agrformet.2010.11.010.

Karl, T., P. Harley, L. Emmons, B. Thornton, A. Guenther, C. Basu, A. Turnipseed, and K. Jardine (2010), Efficient atmospheric cleansing of oxidized organic trace gases by vegetation, *Science*, *330*, 816–819, doi:10.1126/science.1192534.

Meyers, T. P., P. Finkelstein, J. Clarke, T. G. Ellestad, and P. F. Sims (1998), A multilayer model for inferring dry deposition using standard meteorological measurements, *J. Geophys. Res.*, *103*(D17), 22,645–22,661, doi:10.1029/98JD01564.

Mitchell, K. E., et al. (2004), The multi-institution North American Land Data Assimilation System (NLDAS): Utilizing multiple GCIP products and partners in a continental distributed hydrological modeling system, *J. Geophys. Res.*, *109*, D07S90, doi:10.1029/2003JD003823.

Moxim, W. J., H. Levy II, and P. S. Kasibhatla (1996), Simulated global tropospheric PAN: Its transport and impact on NO_x, *J. Geophys. Res.*, *101*(D7), 12,621–12,638, doi:10.1029/96JD00338.

Niyogi, D. S., and S. Raman (1997), Comparison of four different stomatal resistance schemes using FIFE observations, *J. Appl. Meteorol.*, *36*(7), 903–917, doi:10.1175/1520-0450(1997)036<0903:COFDSR>2.0.CO;2.

Niyogi, D. S., K. Alapaty, S. Raman, and F. Chen (2009), Development and evaluation of a coupled Photosynthesis-Based Gas Exchange Evapotranspiration Model (GEM) for mesoscale weather forecasting applications, *J. Appl. Meteorol. Climatol.*, *48*(2), 349–368, doi:10.1175/2008JAMC1662.1.

Palmroth, S., C. A. Maier, H. R. McCarthy, A. C. Oishi, H. S. Kim, K. H. Johnsen, G. G. Katul, and R. Oren (2005), Contrasting responses to drought of forest floor CO_2 efflux in a Loblolly pine plantation and a nearby Oak-Hickory forest, *Global Change Biol.*, *11*(3), 421–434, doi:10.1111/j.1365-2486.2005.00915.x.

Pleim, J., and L. Ran (2011), Surface flux modeling for air quality applications, *Atmosphere*, *2*, 271–302, doi:10.3390/atmos2030271.

Roberts, J. M., et al. (1996), Episodic removal of NO_y species from the marine boundary layer over the North Atlantic, *J. Geophys. Res.*, *101*(D22), 28,947–28,960, doi:10.1029/96JD02632.

Schrimpf, W., K. Lienaerts, K. P. Muller, J. Rudolph, R. Neubert, W. Schubler, and I. Levin (1996), Dry deposition of peroxyacetyl nitrate (PAN): Determination of its deposition velocity at night from measurements of the atmospheric PAN and ^{222}Radon concentration gradient, *Geophys. Res. Lett.*, *23*, 3599–3602, doi:10.1029/96GL03287.

Schuchmann, M. N., and C. von Sonntag (1988), The hydration of the acetyl radical. A pulse radiolysis study of acetaldehyde in aqueous solution, *J. Am. Chem. Soc.*, *110*, 5698–5701, doi:10.1021/ja00225a019.

Shepson, P. B., J. W. Bottenheim, D. R. Hastie, and A. Venkatram (1992), Determination of the relative ozone and PAN deposition velocities at night, *Geophys. Res. Lett.*, *19*, 1121–1124, doi:10.1029/92GL01118.

Singh, H. B. (1987), Reactive nitrogen in the atmosphere, *Environ. Sci. Technol.*, *21*, 320–327, doi:10.1021/es00158a001.

Singh, H. B., and P. L. Hanst (1981), Peroxyacetyl nitrate (PAN) in the unpolluted atmosphere: An important reservoir for nitrogen oxides, *Geophys. Res. Lett.*, *8*(8), 941–944, doi:10.1029/GL008i008p00941.

Sparks, J. P., J. M. Roberts, and R. K. Monson (2003), The uptake of gaseous organic nitrogen by leaves: A significant global nitrogen transfer process, *Geophys. Res. Lett.*, *30*(23), 2189, doi:10.1029/2003GL018578.

Talukdar, R. K., J. B. Burkholder, A. M. Schmoltner, J. M. Roberts, R. R. Wilson, and A. R. Ravishankara (1995), Investigation of the loss processes for peroxyacetyl nitrate in the atmosphere: UV photolysis and reaction with OH, *J. Geophys. Res.*, *100*(D7), 14,163–14,173, doi:10.1029/95JD00545.

Turnipseed, A. A., L. G. Huey, E. Nemitz, R. Stickel, J. Higgs, D. J. Tanner, D. L. Slusher, J. P. Sparks, F. Flocke, and A. Guenther (2006), Eddy covariance fluxes of peroxyacetyl nitrates (PANs) and NOy to a coniferous forest, *J. Geophys. Res.*, *111*, D09304, doi:10.1029/2005JD006631.

Villalta, P. W., E. R. Lovejoy, and D. R. Hanson (1996), Reaction probability of peroxyacetyl radical on aqueous surfaces, *Geophys. Res. Lett.*, *23*, 1765–1768, doi:10.1029/96GL01286.

Wesely, M. L. (1989), Parameterization of surface resistances to gaseous dry deposition in regional-scale numerical models, *Atmos. Environ.*, *23*, 1293–1304, doi:10.1016/0004-6981(89)90153-4.

Wesely, M. L., and B. B. Hicks (2000), A review of the current status of knowledge in dry deposition, *Atmos. Environ.*, *34*, 2261–2282, doi:10.1016/S1352-2310(99)00467-7.

Wolfe, G. M., and J. A. Thornton (2011), The Chemistry of Atmosphere-Forest Exchange (CAFE) Model—Part 1: Model description and characterization, *Atmos. Chem. Phys.*, *11*, 77–101, doi:10.5194/acp-11-77-2011.

Wolfe, G. M., J. A. Thornton, R. L. N. Yatavelli, M. McKay, A. H. Goldstein, B. LaFranchi, K. E. Min, and R. C. Cohen (2009), Eddy covariance fluxes of acyl peroxy nitrates (PAN, PPN and MPAN) above a Ponderosa pine forest, *Atmos. Chem. Phys.*, *9*, 615–634, doi:10.5194/acp-9-615-2009.

Wolfe, G. M., et al. (2011), The Chemistry of Atmosphere-Forest Exchange (CAFE) Model—Part 2: Application to BEARPEX-2007 observations, *Atmos. Chem. Phys.*, *11*, 1269–1294, doi:10.5194/acp-11-1269-2011.

Wu, Y., B. Brashers, P. L. Finkelstein, and J. E. Pleim (2003), A multilayer biochemical dry deposition model. 1. Model formulation, *J. Geophys. Res.*, *108*(D1), 4013, doi:10.1029/2002JD002293.

Wu, Z. Y., X. M. Wang, F. Chen, A. A. Turnipseed, A. B. Guenther, D. Niyogi, U. Charusombat, B. C. Xia, J. W. Munger, and K. Alapaty (2011), Evaluating the calculated dry deposition velocities of reactive nitrogen oxides and ozone from two community models over a temperate deciduous forest, *Atmos. Environ.*, *45*, 2663–2674, doi:10.1016/j.atmosenv.2011.02.063.

Zhang, L., M. D. Moran, and J. R. Brook (2001), A comparison of models to estimate in-canopy photosynthetically active radiation and their influence on canopy stomatal resistance, *Atmos. Environ.*, *35*, 4463–4470, doi:10.1016/S1352-2310(01)00225-4.

Zhang, L., J. R. Brook, and R. Vet (2002), On ozone dry deposition—With emphasis on non-stomatal uptake and wet canopies, *Atmos. Environ.*, *36*, 4787–4799, doi:10.1016/S1352-2310(02)00567-8.

Zhang, L., J. R. Brook, and R. Vet (2003), A revised parameterization for gaseous dry deposition in air-quality models, *Atmos. Chem. Phys.*, *3*, 2067–2082, doi:10.5194/acp-3-2067-2003.

K. Alapaty, Atmospheric Modeling and Analysis Division, U.S. Environmental Protection Agency, Research Triangle Park, NC 27711, USA.

F. Chen, A. B. Guenther, T. Karl, and A. A. Turnipseed, National Center for Atmospheric Research, Boulder, CO 80307, USA.

L. G. Huey, School of Earth and Atmospheric Sciences, Georgia Institute of Technology, Atlanta, GA 30332, USA.

D. Niyogi, Purdue University, West Lafayette, IN 47907, USA.

X. Wang, Z. Wu, and B. Xia, School of Environmental Science and Engineering, Sun Yat-sen University, Guangzhou 510275, China. (eeswxm@mail.sysu.edu.cn)

L. Zhang, Air Quality Research Division, Science and Technology Branch, Environment Canada, Toronto, ON M3H 5T4, Canada.